

Simultaneous Realization of Dynamic and Hybrid Multiplexed Holography via Light-Activated Chiral Superstructures

Peng Chen,* Zhi-Xiong Shen, Chun-Ting Xu, Yi-Heng Zhang, Shi-Jun Ge, Ling-Ling Ma, Wei Hu,* and Yan-Qing Lu*

As a well-recognized technology for optical data encoding and extracting, holography has faced an ever-growing pursuit in the miniaturization, multifunctionality, and tunability for today's abundant information. Despite infusive achievements in metahologram, simultaneous realization of dynamic tunability and high-dimensional multiplexing is critical yet lagging behind, which becomes one bottleneck for this emerging frontier. Here, an innovative solution is proposed by integrating the limited penetration depth of light in chiral liquid crystals and their intrinsic stimuli-responsive characteristics. Based on a photoactive chiral dopant and the asymmetric photopatterning boundary confined self-organization, light-activated spectrally tunable, polarization- and direction-dependent holograms are created simultaneously. As a promising example for information technology, an encrypted signal light is demonstrated, where the wavelength, propagation direction, helicity of light, and reaction duration serve as customized keys for information decryption. This work extends the construction of soft hierarchical superstructures and offers a satisfactory and open-ended scheme for the intelligent holography, inspiring advanced display, security, and communication.

and even entertainment.^[2] However, traditional holographic elements rely on the phase accumulation along propagation, resulting in bulky configuration, low resolution and serious wavelength dependency. This exploits only a glimpse of opportunities that holography can offer. To satisfy the tendency of photonic integration, metasurface with an ultracompact volume and extraordinary functionality has taken off as a booming topic in recent years.^[3,4] Particularly, a sustaining wave of advances in metahologram has been witnessed from visible, terahertz, to microwave frequencies.^[5,6] To release the capacity and strengthen the security for information processing, versatile smart holographic multiplexing schemes have been invented, including wavelength,^[7,8] polarization,^[9–12] orbital angular momentum,^[13] and nonlinear^[14] multiplexing.


Despite those impressive achievements, some challenging issues persist,

1. Introduction

Effective recording, multiplexing, encryption, and readout of numerous data are prerequisite in modern information society. Originated in last century,^[1] holography has emerged as a vital technique to encoding and reconstructing the entire optical information of certain objects. It can provide a vivid 3D observation for human visual perception and has inspired remarkable applications in 3D display, information technology

especially in the simultaneous realization of dynamic tunability and hybrid multiplexing. On one hand, expanding multiplexed degrees of freedom is urgent. For example, the propagation direction, another intriguing physical dimension of light, has been rarely explored.^[15,16] Creating directional hologram is still elusive. On the other hand, dynamic control of the hologram is key and currently highly sought after. Few efforts have been devoted by employing stretchable substrates,^[17] electrical printed-circuit-board,^[18] phase-transition materials,^[19,20] and controlled chemical reactions.^[21,22] Unfortunately, the stringent requirement and highly sophisticated implementation leave it very tough for the simultaneous realization of actively tunable and high-dimensional holographic multiplexing, especially, at visible regime. In terms of reconfigurable optical devices, liquid crystal (LC) has been identified as one of the most appealing platform.^[23] In particular, cholesteric liquid crystal (CLC) has attracted numerous attention due to its self-assembled chiral photonic crystal and the circular-polarization-selective photonic band gap (PBG).^[24] Lately, planar CLC has been discovered to modulate the reflective geometric phase in a polychromatic and polarization-determined manner.^[24–27] If further exploiting the limited penetration depth of light in CLCs^[28] and introducing

P. Chen, Z.-X. Shen, C.-T. Xu, Y.-H. Zhang, S.-J. Ge, L.-L. Ma, W. Hu, Y.-Q. Lu
National Laboratory of Solid State Microstructures
Key Laboratory of Intelligent Optical Sensing and Manipulation
College of Engineering and Applied Sciences
and Collaborative Innovation Center of Advanced Microstructures
Nanjing University
Nanjing 210093, China
E-mail: chenpeng@nju.edu.cn; huwei@nju.edu.cn; yqlu@nju.edu.cn

 The ORCID identification number(s) for the author(s) of this article can be found under <https://doi.org/10.1002/lpor.202200011>

DOI: 10.1002/lpor.202200011

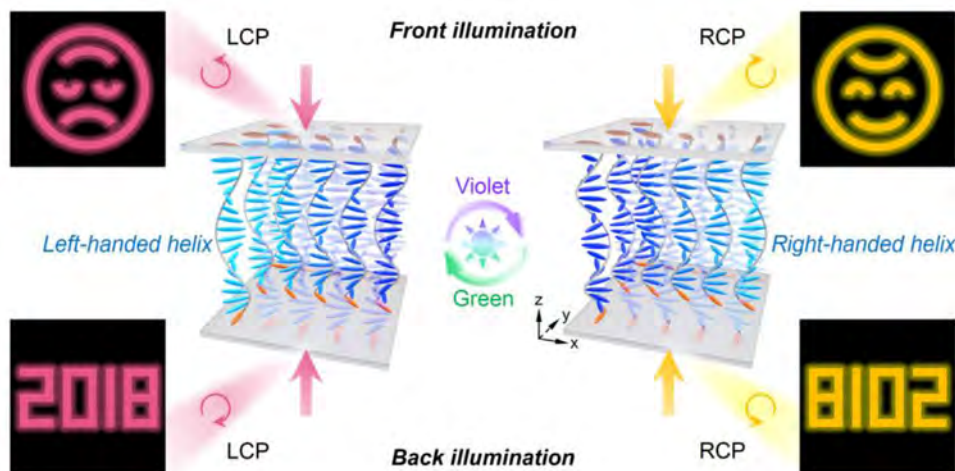


Figure 1. Schematics of the dynamic and hybrid multiplexed holography. Opposite handedness of chirality invertible liquid-crystalline superstructures driven by the violet and green light is labeled respectively, with a centrosymmetric reconstructed image. The red/yellow arrows indicate the incident and reflected light with distinct wavelengths. The LC directors adjacent to the superstrate and substrate are highlighted in orange. LCP, left circular polarization; RCP, right circular polarization.

their intrinsic stimuli-responsive characteristics,^[29–31] hybrid multiplexed hologram simultaneously encoded with bidirectional functionality and dynamic tunability could be expected.

In this work, we propose the light-activated hybrid-multiplexed holography at visible region based on a chirality invertible liquid-crystalline superstructure. By incorporating a photosensitive chiral molecule with the asymmetric photopatterning boundary, high-quality propagation-direction-dependent images are reconstructed in tunable broadband with high efficiency. The light-triggered reversible switching between centrosymmetric holographic images (e.g., smiling or crying face) is also verified with high sensitivity to the illuminating circular polarization. Such a new methodology integrates several multiplexing schemes into a single device, facilitating the advanced holographic display, high-capacity information storage, and high-security encryption. As a promising example for information technology, an encrypted signal light is further demonstrated with variable independent encoding channels.

2. Results and Discussion

2.1. Design Principle

Planar CLCs induced circular-polarization-selective PBG is exhibited between $n_o p$ and $n_e p$, where p is the helical pitch and n_o/n_e is the ordinary/extraordinary refractive index, respectively. Circularly polarized light with the same handedness as the CLC superstructures is totally reflected, while the orthogonal one gets transmitted. Considering the inhomogeneous alignment, an extra geometric phase will be endowed into the reflected light, which is twice the local entrance-surface orientation angle of CLCs and shows a chirality-determined sign.^[27,32,33] Meanwhile, the transmitted light just experiences a uniform phase shift without local geometric phase modulation.^[24,27] This supplies a promising platform for the polarization-controlled, broadband, and pure-phase holography. It should also be noticed that the reflected light within the PBG decays exponentially inside the CLCs.^[28]

Therefore, asymmetry orientations can be imprinted into the initial and terminal directors of sufficiently thick CLCs, making the propagation-direction-dependent beam shaping achievable. Here, to realize an active multiplexed hologram, we further exploit these fantastic optical properties with versatile stimuli responsiveness of this soft matter. The helical pitch and even the handedness of CLCs are sensitive to electric field, thermal treatment, and light irradiation. For instance, a light-directed chirality invertible liquid-crystalline superstructure is introduced in this work.

Figure 1 schematically illustrates the proposed dynamic and hybrid multiplexed holography. At the beginning, the left-handed CLCs encoded with asymmetry alignment reflect left circular polarization (LCP), and bidirectional holographic images (e.g., crying face and “2018”) are reconstructed upon opposite-direction illumination. While, right circular polarization (RCP) is wholly transmitted and no image is generated owing to the absence of the geometric phase modulation for the transmission.^[24,27] Via the violet light stimulating, original chiral superstructures gradually reverse to be right handed, accompanied with a continuously tunable PBG. Accordingly, RCP with desired working band is reflected and the sign of the geometric phase modulation is flipped from + to –. In this case, the centrosymmetric images (e.g., smiling face and “8102”) are generated respectively. By pumping violet or green light, such optically addressable hologram is reversible. This design integrates several multiplexing schemes into a single hologram, including the propagation direction, the helicity, the wavelength of incident light, and the time of the external stimulus (i.e., reaction duration).

2.2. Light-Activated Hybrid Holographic Multiplexing

The desired chirality invertible CLC superstructures can be obtained by doping a static dopant R5011 and an azobenzene chiral molecule ChAD-3C-S with opposite chirality into a nematic host.^[29] Due to the lack of photoisomerizable groups, the optical absorption spectrum of R5011 exhibits no observable change

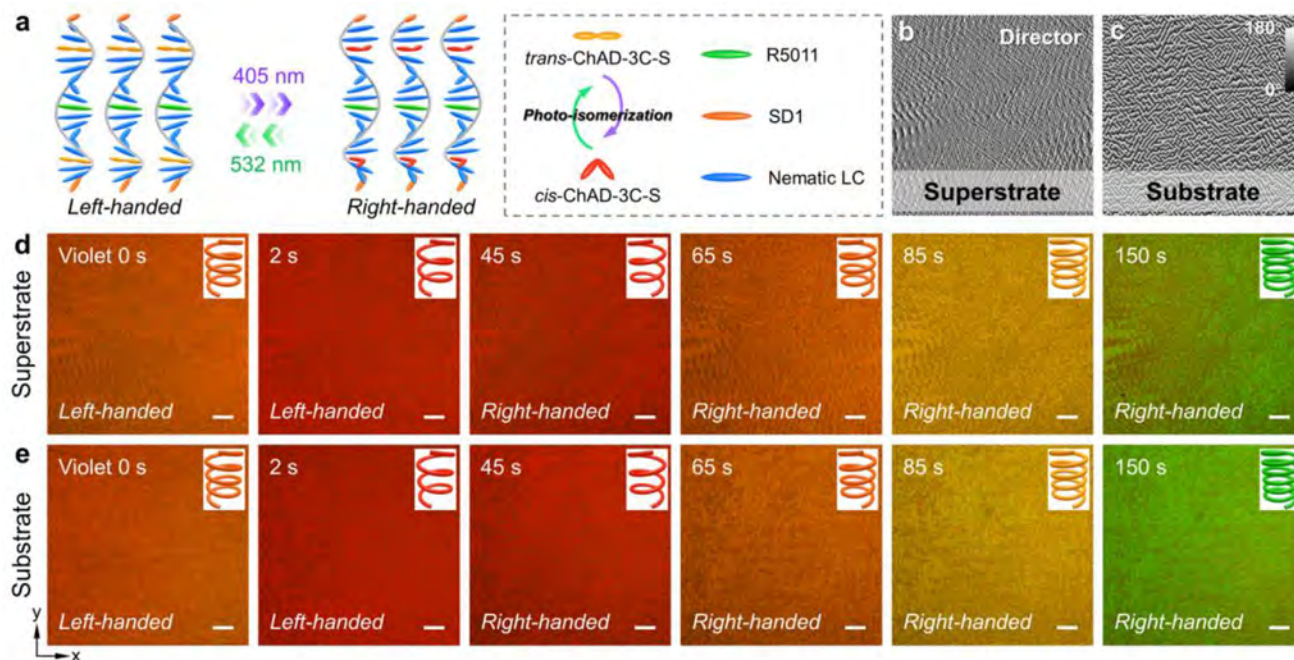


Figure 2. Components and images of the dynamic CLC hologram. a) Mechanism illustration of the light-directed chirality inversion of ChAD-3C-S and R5011 mixture. Inset: Schematic illustration of the photoisomerization reaction of ChAD-3C-S. b,c) Theoretical director distribution and d,e) reflective images of the b,d) superstrate and c,e) substrate, respectively. The color variation from black to white indicates the orientation varying from 0° to 180°. The irradiation time of violet light and real-time chirality are labeled successively. All scale bars are 100 μm .

upon violet light irradiation.^[34] While, ChAD-3C-S is sensitive to violet and green light, which can be verified by its absorption spectra (Figure S1, Supporting Information). Upon pumping light irradiation, the helical pitch of CLC superstructure is continuously tuned and the handedness is reversibly inverted due to the photoisomerization reaction of ChAD-3C-S, as vividly illustrated in **Figure 2a** and verified by corresponding variant transmission spectra (Figure S2, Supporting Information). As the first example, two images with the crying face and Arabic numbers “2018” (see original images in Figure S3, Supporting Information) are respectively encoded into the front and back face of the CLC hologram. Both phase profiles are calculated using the classical Gerchberg–Saxton (GS) algorithm,^[35] which is widely applied in the phase-only holography. To avoid the influence of the zeroth order on the reconstructed image, an off-axis design is adopted and thus the signal-to-noise ratio can be dramatically increased. Referring to the principle of the CLC reflective geometric phase, the required director distributions on superstrate (Figure 2b) and substrate (Figure 2c) can be retrieved by just multiplying 0.5 to respective GS phases (Figure S3, Supporting Information).

To imprint the designed space-variant directors into the superstrate and substrate of the CLC hologram, the photoalignment technique is employed thanks to its fantastic capability of precise LC patterning.^[23] Two substrates spin-coated with the polarization-sensitive photoalignment agent SD1 are independently exposed with different patterns (see details in Note S1, Supporting Information) and then assembled to form a 12 μm thick cell. After infiltrated into the asymmetrically photopatterned cell, the initial and terminal orientations of CLC helices

are controlled by adjacent SD1 on superstrate and substrate, respectively. Owing to the intrinsic viscoelastic property, CLCs can fast self-organize into the guided structure by properly relaxing their chiral superstructures. Figure 2d,e presents the reflective images of the fabricated sample. Some regular disclinations are observed, consistent with the pre-designed orientations. The slight pitch difference may influence the reflected phase, but should be insignificant for a large thickness here.^[28] During the violet light stimulation (405 nm, 8.8 mW cm^{-2}), typical Grandjean textures are exhibited with a uniform brilliant color corresponding to respective PBG (Figure S2, Supporting Information), indicating an ultrabroad working band.

Figure 3a illustrates the experimental setup to characterize the performance of the CLC hologram. To investigate its polychromatic and polarization-selective behavior, a supercontinuum laser, acousto-optic tunable filter, combined with the polarizer and quarter-wave plate are used to control the incident wavelength and polarization state, respectively. Reflected diffraction images are projected onto a screen in the far field and captured by a visible camera. Figure 3b,c shows the holographic reconstructions under opposite illumination directions. As predicted, only the entrance chiral superstructures up to certain penetration depth can affect the reflected light, and the counter face is almost invisible. Before the violet light stimulation, distinct high-quality images (i.e., crying face and “2018”) without any overlapping or distortion are generated on the incidence of LCP, matching well with the theoretical calculation (Figure S3, Supporting Information). The conversion efficiency, defined as the intensity ratio of the reconstructed image to the total reflection, is measured up to 66%, which benefits from the pure phase modulation. While

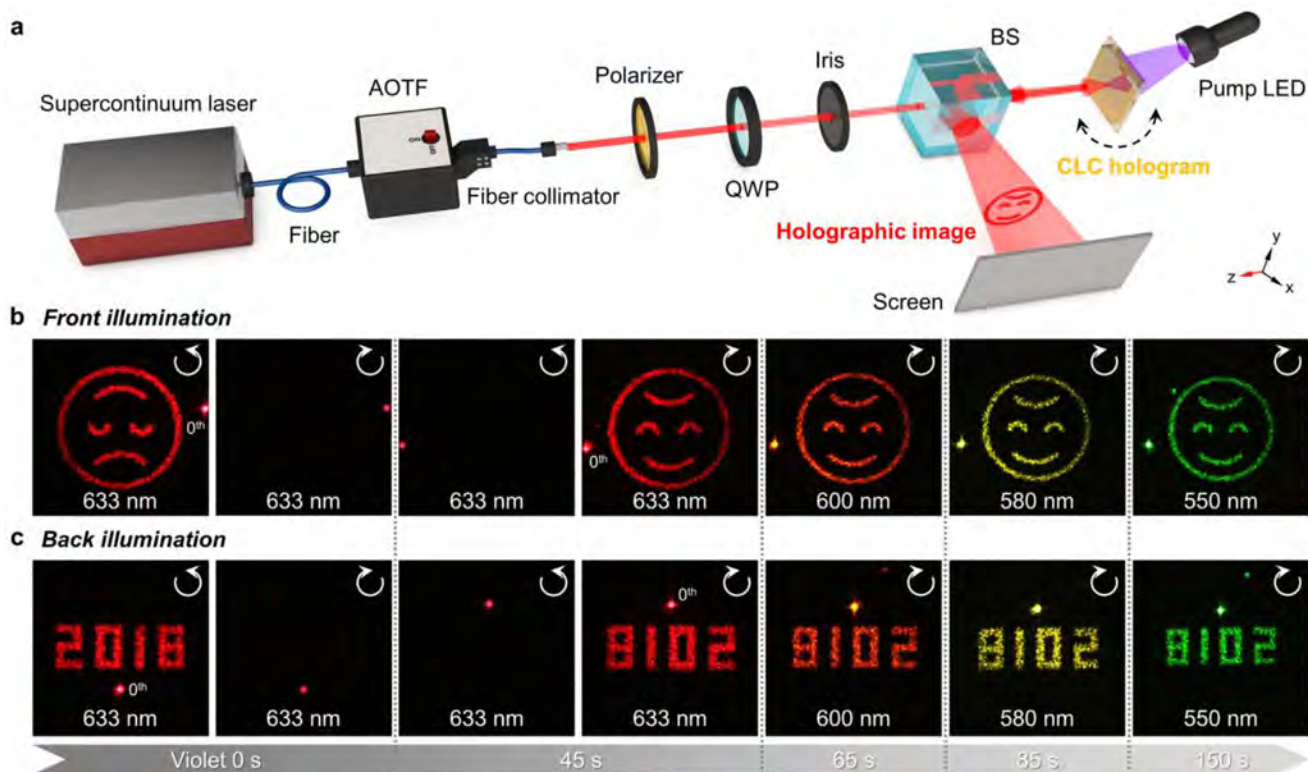


Figure 3. Optical characterization of the dynamic CLC hologram. a) The optical setup. AOTF, acousto-optic tunable filter; QWP, quarter-wave plate; BS, nonpolarizing beam splitter. b,c) Reflected diffraction images at different violet light irradiation time under b) front and c) back illumination. The wavelength and polarization state of the incident light are labeled successively, with clockwise/counterclockwise indicating RCP/LCP.

for RCP, only a weak spot can be observed, mainly attributed to the Fresnel reflection. After chirality inversion of the CLC superstructures, RCP is reflected and experiences a conjugated phase profile, contributing to a symmetrically distributed off-axis image with high fidelity, i.e., smiling face and “8102”. The centrosymmetry point is exactly the location of the zeroth-order reflected light. Along with the violet light irradiation, the available spectral band shifts from near-infrared to green region. It should be mentioned that the image size increases linearly with the imaging distance and the modulated wavelength. For the linearly polarized incident light, the circular polarization component with the same chirality as the CLC is reflected and contributes to a holographic image, while the opposite one transmits and features as a bright spot (see experimental reflection and transmission images of the CLC hologram in Figure S4, Supporting Information).

2.3. Optical Information Encryption

Optical cryptography has become one of the most significant methods for information security and anticounterfeiting technology, thanks to its inherent capability of combining numerous independent encoding channels and thus enhancing the security level. Here, the realization of high-dimensional holographic multiplexing in a photoreversible manner will definitely facilitate the advanced optical information processing and encryption.

As a proof-of-principle application, an encrypted signal light is delicately designed and demonstrated in **Figure 4**. Four direction messages of the traditional signal light (Figure 4a) are all encrypted into one CLC device (Figure 4b) and sent to multiple receivers. Upon receipt, one can decrypt it and read out distinct signals according to the customized keys, which are composed of specific information about the irradiation time, wavelength, helicity, and propagation direction. As shown in Figure 4c–f, such an identical sample can be extracted into different holographic images, that is, deciphered into manifold messages with respective keys. For instance, *Key 2* of violet 2 s, 650 nm, LCP and front illumination uncovers a red rightward arrow (Figure 4d), which means “Do not turn right!”. *Key 4* gives rise to a green leftward arrow (Figure 4f), indicating “Go left!”. Besides, many other images with complex information, including Morse codes and letters, can be encrypted and decrypted, presenting a high-density and high-security method for the information storage and processing.

The conversion efficiency and the speckle noise accompanied with the pure-phase hologram can be improved by adopting the high-resolution photopatterning systems^[36] and optimized numerical algorithms.^[37] Compared with other stimuli, the light control is usually more desirable due to the superiorities of convenient wireless-operation, noninvasiveness, and high remote-resolution. The response time of these holograms can reach second scale under intense-light irradiation. This satisfies

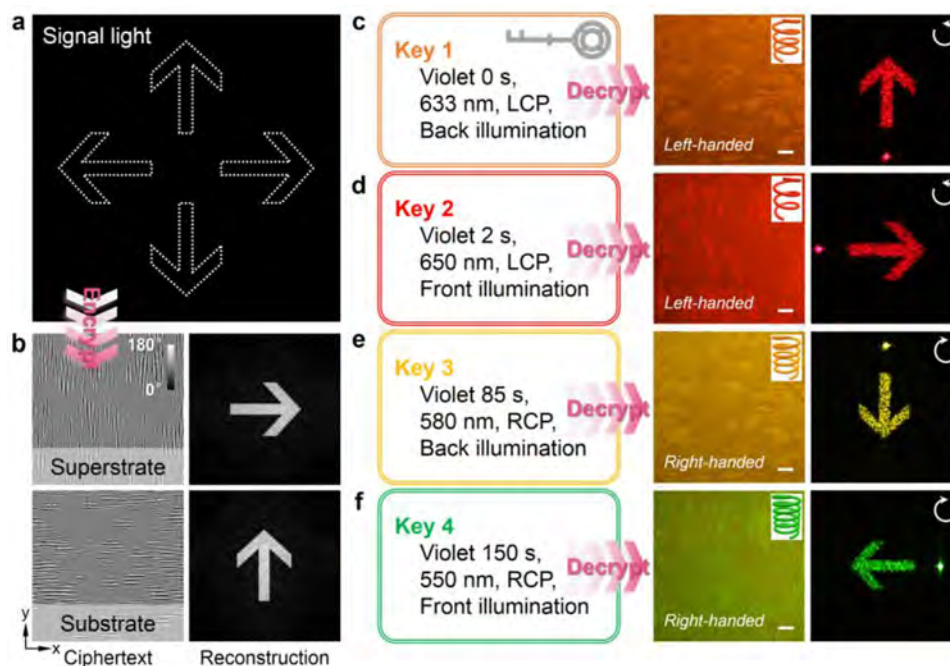


Figure 4. Encrypted signal light. a) Schematic illustration of a traditional signal light. b) The desired director distributions on the superstrate and substrate of the CLC ciphertext and their theoretical reconstructions. The color variation from black to white indicates the orientation varying from 0° to 180° . c–f) Different customized keys and respective decrypted optical information, with real-time chirality and the circular-polarization state labeled in each image and reflected diffraction image. All scale bars are $100 \mu\text{m}$.

the requirement of proof-of-concept demonstration for potential applications, but is challenging to be significantly improved because the whole helical structure with azo-chiral molecules has to gradually unwind. Other stimuli-responsive materials, such as electrically tuned CLCs, are strong candidates to further accelerate the switching process for some practical applications. Via further introducing chiral dopants with weak thermal relaxation and degradation^[38,39] and optimizing the package, the stability and repeatability could be significantly extended. Other chiral photonic structures can be employed as well. For instance, the heliconic CLCs^[40,41] may bring in more degrees of freedom with both phase and amplitude modulation, while stacking several ferroelectric-LC-doped CLCs^[42] can create ultrabroadband dynamic holograms. Benefiting from the rewritability of the photoalignment agent, reconfigurable holography can be rationally anticipated through surface pattern engineering. Moreover, asymmetric boundary induced direction-dependent functionality enriches the dimension for multiplexing and may further boost nonreciprocal planar optical apparatuses. In addition to the all-LC elements demonstrated here, the integration of LCs and fantastic metasurfaces is another promising way to active light control and information decryption.^[43–45]

3. Conclusion

In summary, we demonstrated a new scheme for the dynamic and hybrid multiplexed holography via a light-driven chirality invertible liquid-crystalline superstructure. The collaboration of rapid self-organization confined by asymmetric boundary and the

intrinsic external-stimuli responsivity promotes the hologram engineering to an unprecedented level. Spectrally tunable, helicity selective, and bidirectional visible holograms are generated with merits of high quality, high efficiency and good reversibility. As a proof-of-principle application, an encrypted signal light is presented and can be decrypted into customized direction messages. This work deals with several critical issues associated with current static metaholography and may be a satisfactory solution to the simultaneous realization of dynamic and high-dimensional multiplexing in a single hologram. Such a novel and open-ended strategy is a vital step forward and may inspire versatile applications in holographic display, high-capacity, and high-security information technology.

4. Experimental Section

Materials: The light-activated chiral liquid-crystalline superstructure was prepared by mixing a nematic LC (HTW114200-050, HCCH, China) with 3.1 wt% right-handed chiral dopant (R5011, HCCH, China) and 12 wt% left-handed azobenzene chiral molecule (ChAD-3C-S, BEAM Co., USA). Upon violet light irradiation, the molecules of ChAD-3C-S sequentially isomerize from the rod-like *trans*-form to the bend *cis*-form structure (Figure 2a) and its helical twisting power drops gradually. In the absence of light stimulus, the opposite *cis*-*trans* isomerization is slow but can be drastically accelerated by green light irradiation. A polarization-sensitive sulfonic azo-dye SD1 (Dai-Nippon Ink and Chemicals, Japan) was used as the photoalignment agent, whose molecules tend to reorient their absorption oscillators perpendicular to the polarization direction of the illuminating UV light and further guide LCs.

Sample Fabrication: As revealed in Figure S5 in the Supporting Information, indium-tin-oxide glass substrates ($1.5 \times 2 \text{ cm}^2$) were ultrasonically

bathed, UV-Ozone cleaned, and then spin-coated with the SD1 dissolved in dimethylformamide at a concentration of 0.3 wt%. After curing at 100 °C for 10 min, two pieces of glass substrates were independently placed at the image plane of the digital-micromirror-device-based microlithography system (Figure S6, Supporting Information). Briefly, the director distribution of each hologram is calculated and divided into 36 sub-regions endowed from 0° to 175° in the interval of 5°. A sum of five adjacent sub-regions is exposed simultaneously and the subsequent exposure shifts one sub-region with the polarizer rotating 5° synchronously. Finally, each sub-region is exposed five times with a total exposure dose of $\approx 5 \text{ J cm}^{-2}$. Through such 36-step five-time partly overlapping exposure process, the designed director distributions can be carried out on the superstrate and substrate, respectively (see Note S1, Supporting Information, for more details). Then, these two substrates were separated by the 12 μm thick Mylar and sealed with epoxy glue to form a cell. The CLC material was capillary-filled into this asymmetrically photopatterned cell at 110 °C and slowly cooled to room temperature.

Characterizations: All experiments were performed at room temperature under ambient environment. All images of the CLC holograms were recorded under the reflective mode of an optical microscope (50i POL, Nikon, Japan). The pumping violet light emitting diode (M405L2, Thorlabs, USA) was at 405 nm and 8.8 mW cm^{-2} . The transmission spectra were measured with a spectrometer (USB4000, Ocean Optics, USA). The supercontinuum fiber laser (SuperK EVO, NKT Photonics, Denmark) was filtered at different monochromatic wavelengths by the multichannel acousto-optic tunable filter (SuperK SELECT, NKT Photonics, Denmark). Reflected diffraction images were captured by a visible digital camera (EOS M, Canon, Japan).

Supporting Information

Supporting Information is available from the Wiley Online Library or from the author.

Acknowledgements

This work was supported by the National Key Research and Development Program of China (No. 2021YFA1202000), the National Natural Science Foundation of China (NSFC) (Nos. 62035008, 62175101, 12004175, 61922038, 52003115, and 62105143), the Natural Science Foundation of Jiangsu Province (Nos. BK20212004, BK20200311, BK20200320, and BK20210179), and the Innovation and Entrepreneurship Program of Jiangsu Province.

Conflict of Interest

The authors declare no conflict of interest.

Data Availability Statement

The data that support the findings of this study are available from the corresponding author upon reasonable request.

Keywords

chiral liquid crystals, geometric phases, holographic multiplexing, information encryption, light-driven superstructures, metaholograms

Received: January 8, 2022

Published online: March 17, 2022

- [1] D. Gabor, *Nature* **1948**, *161*, 777.
- [2] R. Collier, C. B. Buckart, L. H. Lin, *Optical Holography*, Academic, New York **1971**.
- [3] N. Yu, F. Capasso, *Nat. Mater.* **2014**, *13*, 139.
- [4] S. Chen, W. Liu, Z. Li, H. Cheng, J. Tian, *Adv. Mater.* **2020**, *32*, 1805912.
- [5] G. Zheng, H. Mühlenbernd, M. Kenney, G. Li, T. Zentgraf, S. Zhang, *Nat. Nanotechnol.* **2015**, *10*, 308.
- [6] Q. Jiang, G. Jin, L. Cao, *Adv. Opt. Photonics* **2019**, *11*, 518.
- [7] B. Wang, F. Dong, Q. Li, D. Yang, C. Sun, J. Chen, Z. Song, L. Xu, W. Chu, Y. F. Xiao, Q. Gong, Y. Li, *Nano Lett.* **2016**, *16*, 5235.
- [8] X. Li, L. Chen, Y. Li, X. Zhang, M. Pu, Z. Zhao, X. Ma, Y. Wang, M. Hong, X. Luo, *Sci. Adv.* **2016**, *2*, e1601102.
- [9] D. Wen, F. Yue, G. Li, G. Zheng, K. Chan, S. Chen, M. Chen, K. F. Li, P. W. H. Wong, K. W. Cheah, E. Y. B. Pun, S. Zhang, X. Chen, *Nat. Commun.* **2015**, *6*, 8241.
- [10] A. Arbabi, Y. Horie, M. Bagheri, A. Faraon, *Nat. Nanotechnol.* **2015**, *10*, 937.
- [11] J. B. Mueller, N. A. Rubin, R. C. Devlin, B. Groever, F. Capasso, *Phys. Rev. Lett.* **2017**, *118*, 113901.
- [12] L. Deng, J. Deng, Z. Guan, J. Tao, Y. Chen, Y. Yang, D. Zhang, J. Tang, Z. Li, Z. Li, S. Yu, G. Zheng, H. Xu, C. W. Qiu, S. Zhang, *Light: Sci. Appl.* **2020**, *9*, 101.
- [13] X. Fang, H. Ren, M. Gu, *Nat. Photonics* **2020**, *14*, 102.
- [14] G. Li, S. Zhang, T. Zentgraf, *Nat. Rev. Mater.* **2017**, *2*, 17010.
- [15] Y. Chen, X. Yang, J. Gao, *Light: Sci. Appl.* **2019**, *8*, 45.
- [16] K. Chen, G. Ding, G. Hu, Z. Jin, J. Zhao, Y. Feng, T. Jiang, A. Alù, C. W. Qiu, *Adv. Mater.* **2020**, *32*, 1906352.
- [17] S. C. Malek, H. S. Ee, R. Agarwal, *Nano Lett.* **2017**, *17*, 3641.
- [18] L. Li, T. J. Cui, W. Ji, S. Liu, J. Ding, X. Wan, Y. B. Li, M. Jiang, C. W. Qiu, S. Zhang, *Nat. Commun.* **2017**, *8*, 197.
- [19] X. Yin, T. Steinle, L. Huang, T. Taubner, M. Wuttig, T. Zentgraf, H. Giessen, *Light: Sci. Appl.* **2017**, *6*, e17016.
- [20] F. Zhang, X. Xie, M. Pu, Y. Guo, X. Ma, X. Li, J. Luo, Q. He, H. Yu, X. Luo, *Adv. Mater.* **2020**, *32*, 1908194.
- [21] J. Li, S. Kamin, G. Zheng, F. Neubrech, S. Zhang, N. Liu, *Sci. Adv.* **2018**, *4*, eaar6768.
- [22] J. Li, Y. Chen, Y. Hu, H. Duan, N. Liu, *ACS Nano* **2020**, *14*, 7892.
- [23] P. Chen, B. Y. Wei, W. Hu, Y. Q. Lu, *Adv. Mater.* **2020**, *32*, 1903665.
- [24] J. Kobashi, H. Yoshida, M. Ozaki, *Nat. Photonics* **2016**, *10*, 389.
- [25] M. Rafayelyan, G. Tkachenko, E. Brasselet, *Phys. Rev. Lett.* **2016**, *116*, 253902.
- [26] R. Barboza, U. Bortolozzo, M. G. Clerc, S. Residori, *Phys. Rev. Lett.* **2016**, *117*, 053903.
- [27] P. Chen, L. Ma, W. Duan, J. Chen, S. Ge, Z. Zhu, M. Tang, R. Xu, W. Gao, T. Li, W. Hu, Y. Q. Lu, *Adv. Mater.* **2018**, *30*, 1705865.
- [28] J. Kobashi, H. Yoshida, M. Ozaki, *Sci. Rep.* **2017**, *7*, 16470.
- [29] P. Chen, L. L. Ma, W. Hu, Z. X. Shen, H. K. Bisoyi, S. B. Wu, S. J. Ge, Q. Li, Y. Q. Lu, *Nat. Commun.* **2019**, *10*, 2518.
- [30] M. Sadati, J. Martinez-Gonzalez, Y. Zhou, N. T. Qazvini, K. Kurtenbach, X. Li, E. Bokusoglu, R. Zhang, N. L. Abbott, J. Hernandez-Ortiz, J. J. de Pablo, *Sci. Adv.* **2020**, *6*, eaba6728.
- [31] S. U. Kim, Y. J. Lee, J. Liu, D. S. Kim, H. Wang, S. Yang, *Nat. Mater.* **2022**, *21*, 41.
- [32] M. Rafayelyan, E. Brasselet, *Phys. Rev. Lett.* **2018**, *120*, 213903.
- [33] Y. Li, T. Zhan, Z. Yang, C. Xu, P. L. LiKamWa, K. Li, S. T. Wu, *Opt. Express* **2021**, *29*, 6011.
- [34] L. Wang, D. Chen, K. G. Gutierrez-Cuevas, H. K. Bisoyi, J. Fan, R. S. Zola, G. Li, A. M. Urbas, T. J. Bunning, D. A. Weitz, Q. Li, *Mater. Horiz.* **2017**, *4*, 1190.
- [35] R. W. Gerchberg, W. O. Saxton, *Optik* **1972**, *35*, 237.
- [36] Y. Guo, M. Jiang, S. Afghah, C. Peng, R. L. B. Selinger, O. D. Lavrentovich, Q. H. Wei, *Adv. Opt. Mater.* **2021**, *9*, 2100181.
- [37] H. Ren, W. Shao, Y. Li, F. Salim, M. Gu, *Sci. Adv.* **2020**, *6*, eaaz4261.

- [38] Z. G. Zheng, Y. Li, H. K. Bisoyi, L. Wang, T. J. Bunning, Q. Li, *Nature* **2016**, *537*, 352.
- [39] L. Qin, W. Gu, J. Wei, Y. Yu, *Adv. Mater.* **2018**, *30*, 1704941.
- [40] J. Xiang, Y. Li, Q. Li, D. A. Paterson, J. M. D. Storey, C. T. Imrie, O. D. Lavrentovich, *Adv. Mater.* **2015**, *27*, 3014.
- [41] C. L. Yuan, W. Huang, Z. G. Zheng, B. Liu, H. K. Bisoyi, Y. Li, D. Shen, Y. Q. Lu, Q. Li, *Sci. Adv.* **2019**, *5*, eaax9501.
- [42] S. Jiang, C. C. Lai, Y. S. Zhang, J. D. Lin, W. C. Lin, X. L. Hsieh, C. R. Lee, *Adv. Opt. Mater.* **2021**, *9*, 2100746.
- [43] M. Sharma, T. Ellenbogen, *Laser Photonics Rev.* **2020**, *14*, 2000253.
- [44] K. Li, J. Wang, W. Cai, H. He, M. Cen, J. Liu, D. Luo, Q. Mu, D. Gérard, Y. J. Liu, *Nano Lett.* **2021**, *21*, 7183.
- [45] J. Wang, K. Li, H. He, W. Cai, J. Liu, Z. Yin, Q. Mu, V. K. S. Hisao, D. Gérard, D. Luo, G. Li, Y. J. Liu, *Laser Photonics Rev.* **2022**, *16*, 2100396.